IET Generation, Transmission & Distribution

Special Issue: Optimal Utilisation of Storage Systems in Transmission and Distribution Systems

IET Journals
The Institution of Engineering and Technology

Optimal design of battery energy storage system for a wind–diesel off-grid power system in a remote Canadian community

ISSN 1751-8687
Received on 3rd February 2015
Revised on 29th May 2015
Accepted on 16th June 2015
doi: 10.1049/iet-gtd.2015.0190
www.ietdl.org

Li Guo[1] ✉, Zhouzi Yu[1], Chengshan Wang[1], Fangxing Li[2], Jean Schiettekatte[3], Jean-Claude Deslauriers[3], Lingquan Bai[2]

[1]*Key Laboratory of Smart Grid of Ministry of Education, Tianjin University, Tianjin 300072, People's Republic of China*
[2]*Department of Electrical Engineering and Computer Science, The University of Tennessee, Knoxville 37996, USA*
[3]*Nimschu Iskudow Inc, Montreal H3V 1A2, Canada*
✉ *E-mail: liguo@tju.edu.cn*

Abstract: This study focuses on the design issue of battery energy storage system (BESS) for a wind–diesel off-grid power system located in the Whapmagoostui community in Quebec, Canada. The local range of wind speed is from 0 to 24.8417 m/s, and the total yearly load demand in 2013 was 11,176 MWh. An optimal planning model is proposed in this study with the objectives of maximising the economic, environmental benefits, and reliability of the system. The battery energy capacity and the rated capacity of converter are selected as the optimal variables. In order to consider the impacts of renewable energy randomness, the uncertainty of component failures, and the power flow constraints on planning results, quasi-steady state simulation is adopted to calculate the indices for each design scheme of BESS. The proposed optimal planning model of BESS is implemented and verified in the Whapmagoostui community. Also, a detailed analysis of several scenarios is presented. A base scenario with three diesel generators and four wind turbines is investigated, and its optimal BESS integration reduces fuel consumption by 4% and improves the average annual profit by 19%. The optimal designing of BESS enhances the economic, environmental benefits, and reliability of the wind–diesel system with high fuel prices in the Whapmagoostui community.

1 Introduction

As defined by Natural Resources Canada, an off-grid community is 'a permanent or long-term settlement that is neither connected to the North American electrical grid nor to the piped natural gas network.' There are more than 175 aboriginal and northern off-grid communities across Canada, and most of them rely primarily on diesel generators (DGs) for the electricity supply [1]. Approximately 100,000 people live in these communities, where the average unsubsidised price for electricity is approximately C$1.3/kWh, including communities as far north as Nunavut [2]. For the diesel generation, the electricity costs of these communities are much higher than the rest of Canada, which ranges from C$0.07 to C $0.17/kWh, and vary significantly depending on the communities' transportation access [3]. The high fuel prices and serious pollutant emissions of diesel generation have become a limiting factor that impedes the development of economy and residential living standards in these off-grid communities.

However, Canada has a huge potential for renewable energy resources (RER), such as wind and biomass [4]. Therefore, the Aboriginal Affairs and Northern Development Canada proposed the 'Aboriginal and Northern Community Action Program' from 2003–2007 and the subsequent 'ecoENERGY for Aboriginal and Northern Communities Program' in 2007 to make full use of the local RER in remote communities and reduce diesel fuel consumption [5]. This situation is quite similar to Alaska, where the Alaska State Legislature started and funded the Renewable Energy Fund grant program in 2008 [6]. Several wind–diesel projects in Alaska have been proven to be successful, such as St. Paul's Island with a single 225 kW wind turbine (WT), and Wales installed two WTs with a total capacity of 100 kW [7]. In the UK, the wind–diesel system is also chosen as an alternative for remote farm areas like North Canterbury [8]. Therefore, it is a feasible alternative to constitute a wind–diesel off-grid power system to reduce diesel fuel consumption in the remote Canadian communities.

To mitigate the impact renewable energy integration, the battery energy storage system (BESS) is introduced into the off-grid system. The optimal planning of the system should take into account the coordinated control and operation strategy of multiple distributed generators as well as BESS [9, 10]. The work in [11, 12] proposed a multi-objective optimisation model with economic, environmental, and reliability property for a standalone wind–photovoltaic–diesel–battery system, and utilised a multi-objective genetic algorithm to obtain the optimal allocation of power supply. To overcome the difficulty with finding the global optimum of the non-smooth cost function, a matrix real-coded genetic algorithm framework was presented in [13] to solve the optimal allocation problem of distributed generators and storage units in a standalone microgrid. In order to investigate the effects of uncertain factors affecting optimisation results, a stochastic chance-constraint programming model was presented in [14]. In the model, the total net present cost and pollutant emission in life cycle were chosen as the objective function, and the loss of capacity is adopted as the probability index constraint. However, the literatures above only take active power balance as one of their operation constraints. The impact of both active and reactive power balances on bus voltages should be further analysed due to the high resistance of distribution lines in the off-grid system.

Specifically, for the optimal design problem of BESS, recent researches have carried out design work on both capacity and location of BESS in distribution systems [15]. In [16], a methodology for optimal allocation of BESS in a distribution system with high wind energy penetration was presented. The objective was to minimise the annual cost of the electricity, and the constraint was that the system should accommodate all spilled wind energy. A cost-effective evaluation model incorporating an optimal load shedding strategy was proposed in [17] to determine optimal energy storage installation. The costs of energy storage were optimised with respect to system reliability. The authors in [18] investigated the reduction of power loss and deferral of network

upgrading with BESS integrated in distribution systems. With the objective of minimising system costs, genetic algorithm, and sequential quadratic programming were adopted to solve the optimal placement and sizing problem of BESS. The integration of BESS can increase the utilisation rate of RER, reduce the adverse impact of RER on network voltage and improve the reliability of system. However, the literature above did not consider simultaneously the random property of the RER and the uncertainty of components' forced outage.

This paper proposes an optimal planning method of BESS for a wind–diesel off-grid power system of the Whapmagoostui community in Quebec, Canada. Firstly, the operation strategy of BESS in an off-grid system is investigated and a variety of BESS's functions are discussed. Secondly, an optimal planning model aiming at maximising economic, environmental, and reliability benefits of the system is established. In the proposed model, the battery capacity and converter capacity are selected as optimal variables. The quasi-steady-state simulation is conducted to analyse different planning schemes considering the randomness of RER, uncertainty of components' failure and power flow constraints. Finally, optimal planning of BESS in the Whapmagoostui community is carried out by the proposed model, and the effects of BESS's integration are analysed.

This work is organised as follows. In Section 2, the operation strategy and function of BESS are introduced. In Section 3, the proposed optimal planning model is presented. In Section 4, a case study for the Whapmagoostui community's off-grid system is performed. Section 5 provides the conclusion of this paper.

2 BESS operation strategies in an off-grid system

There are various operation strategies of BESS for different system configurations. Since this work focuses on applying BESS to a wind–diesel off-grid system, only the coordinated control strategies considering both BESS and DGs are investigated. The strategies can be divided into two categories [19]: (i) DGs work as the main power supply to follow the net load demand and (ii) BESS takes the primary responsibility for meeting the net load demand. The net load demand equals the total load demand minus the output power of renewable energy generation.

In the first category, most of the net load demand is offset by DGs. BESS only compensates the part of the net load demand that exceeds the capability of DGs, thus BESS basically operating under floating charge conditions. It can be envisioned that the BESS acts more as a back-up power source to increase the reserve capacity and enhance the reliability level of the system. In the second category, the DGs and BESS take turns to be main power supply to meet the net load demand. The BESS is able to operate independently so that all DGs in the system can be shut off when the renewable energy generation is sufficient. In this situation, the surplus renewable energy generation can be stored in the BESS and then be discharged during the peak load hours.

Moreover, the grid-connected converter of BESS enables a fast control of reactive power [20]. The converter works in the voltage control mode to keep the voltage constant when the BESS is fully responsible for the voltage regulation. When the DGs play the role of main power supply, the converter provides the part of reactive power that exceeds the capability of DGs. Due to the limited generation capacity of the off-grid system, the ability of the converters to provide reactive power is of great significance and should be taken in the BESS design stage.

3 BESS capacity optimal planning model

3.1 Framework of the optimal planning model

As shown in Fig. 1, the proposed optimal planning model can be divided into the optimal planning module and the quasi-steady-state simulation module. In this model, the randomness of RER, uncertainty of components' failure and power flow constraints are all included in the process of solving the optimization model. In the optimization procedure, first, the optimal planning model pre-determines the objective function, constraint conditions and optimal variables. Then the quasi-steady state simulation is conducted under the constraints for each established BESS design scheme to obtain the operation cost and relative equipment statistics. Finally, the simulation results are delivered to the optimal planning module, and then the objective functions can be acquired by economic evaluation.

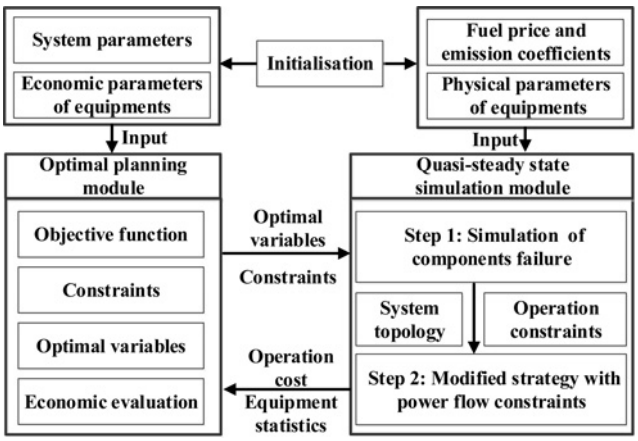

Fig. 1 *Framework of the proposed optimal planning model of BESS*

Compared to existing methods for BESS optimal planning and design, the proposed method has the following three features:

Randomness of RER and load: The intermittent property of the RER and the stochastic feature of load fluctuations have a direct influence on the generation–demand balance in an off-grid system. In this paper, the random properties of wind and load are simulated in the same way as [14]. Wind speed is assumed to follow the Weibull distribution and time series wind data is generated by the Markov process transition probability matrix. Load data is obtained by the original hourly data multiplied by the load disturbance factor which follows the normal distribution.

Component failure rate: Compared to a large power system, the reserve capacity of an off-grid system is so limited that the failure events of components have a significant impact on system operation. However, the existing methods commonly separate the reliability evaluation from the operation simulation and ignore the fact that the evaluation indices, such as fuel consumption and pollutant emissions, are affected by the forced outage events. To solve the problem, reliability assessment is incorporated into the quasi-steady state simulation in this paper. The simulation period is controlled by the convergence of reliability index.

Various functions of BESS: In an off-grid system, BESS can shift peak load, increase wind energy utilization rate and improve power supply reliability. In addition, the grid connected converter of BESS can control reactive power simultaneously to maintain a constant bus voltage, especially when the reactive capacity of DGs is insufficient. In order to take various functions of BESS into account, a modified strategy with power flow constraints is proposed in this paper.

3.2 Optimal planning mathematical model

3.2.1 Objective function: Economic, environmental friendliness, and reliability are the three most important evaluation indices for an off-grid power system. In this paper, internal rate of return (IRR), life cycle pollutant emissions, and loss of energy expectation (LOEE) are selected as the economic, environmental, and reliable indices, respectively. The three conflicting indices can be formulated as a single objective function by introducing the weighted sum method [21], in which the values for weighting coefficients reflect the global preference information of the

decision-maker. The objective function is formulated as

$$f = \min(-\varpi_1 \mathrm{IRR}' + \varpi_2 C_{\mathrm{p}}' + \varpi_3 \mathrm{LOEE}') \quad (1)$$

where IRR', C_{p}', and LOEE' are the IRR, pollutant emissions and the LOEE of the project after normalisation, respectively; and ϖ_1, ϖ_2, and ϖ_3 are the weighting coefficients of corresponding indices. The negative value of IRR is used in the objective function to maximise the system profit.

(i) *IRR*: It is the discount rate to make the net present cost equal to zero. This index reflects the profitability of a project and can be expressed as

$$\sum_{k=1}^{L} [C(k) \times (\mathrm{IRR})]^k = I_0 \quad (2)$$

where I_0 is the initial capital cost of the off-grid system, L is the life cycle of the project, and $C(k)$ is the total cost of the kth year, which can be calculated as follows:

$$C(k) = C_{\mathrm{I}}(k) - C_{\mathrm{R}}(k) - C_{\mathrm{M}}(k) - C_{\mathrm{F}}(k) - C_{\mathrm{D}}(k) + C_{\mathrm{B}}(k) \quad (3)$$

where $C_{\mathrm{I}}(k)$, $C_{\mathrm{R}}(k)$, $C_{\mathrm{M}}(k)$, $C_{\mathrm{F}}(k)$, $C_{\mathrm{D}}(k)$, and $C_{\mathrm{B}}(k)$ are the initial investment cost, replacement cost, operation and maintenance (O&M) cost, fuel cost, depreciation cost, and salvage value in the kth year, respectively.

(ii) *Pollutant emissions*: In this paper, CO, CO_2, unburned hydrocarbon, sulphur compounds, and nitric oxide are considered as pollutant emissions. The pollutant emissions are related to fuel consumption directly, which equal to the life cycle fuel consumption multiplied by the emission coefficient of different pollutants. It can be expressed as [19]

$$C_{\mathrm{e}} = (\sigma^{\mathrm{CO_2}} + \sigma^{\mathrm{CO}} + \sigma^{\mathrm{HC}} + \sigma^{\mathrm{NO}} + \sigma^{\mathrm{S}}) v_{\mathrm{L}}^{\mathrm{fule}} \quad (4)$$

where σ^{CO2}, σ^{CO}, σ^{HC}, σ^{NO}, and σ^{S} are the coefficients of different pollutants, $v_{\mathrm{L}}^{\mathrm{fule}}$ is the diesel consumption in the project life cycle.

(iii) *LOEE*: It reflects the expected power not supplied (PNS) in a setting period. In this paper, the period is set as one year, and the LOEE index can be expressed as

$$\mathrm{LOEE} = \frac{1}{N} \sum_{y=1}^{N} \sum_{t=1}^{8760} H(\mathrm{PNS}_t) \quad (5)$$

where N is the steady-state simulation period, and $H(\mathrm{PNS}_t)$ is the computation function to determine the PNS at the tth time step, which can be expressed as

$$H(\mathrm{PNS}_t) = \begin{cases} \sum_{l \in \mathrm{LP}} \mathrm{PNS}_{l,t}, & \sum_{l \in \mathrm{LP}} \mathrm{PNS}_{l,t} > 0 \\ 0, & \sum_{l \in \mathrm{LP}} \mathrm{PNS}_{l,t} = 0 \end{cases} \quad (6)$$

where $\mathrm{PNS}_{l,t}$ is the PNS of the lth load point at the tth time step, and LP is the set of load points in the system.

It should be noted that no reliability constraint is involved in the proposed model as the system reliability level is formulated as one of the objectives in the objective function, which is similar to the literature [22]. Therefore, there are not any criteria set for LOEE in this paper. The impact of LOEE on the optimisation results is reflected by the corresponding weighting coefficient, which is selected according to the decision-maker's preference on the system reliability level.

3.2.2 Constraints:

(i) Power flow equations

$$\begin{cases} P_{is} = U_i \sum_{j \in i} U_j (G_{ij} \cos \theta_{ij} + B_{ij} \sin \theta_{ij}) \\ Q_{is} = U_i \sum_{j \in i} U_j (G_{ij} \sin \theta_{ij} - B_{ij} \cos \theta_{ij}) \end{cases} \quad (7)$$

where, P_{is} and Q_{is} are the active and reactive power injections of the ith bus, U_i is the voltage magnitude of the ith bus; $j \in i$ denotes all the buses that are directly connected to the ith bus; G_{ij} and B_{ij} are the real and imaginary parts of the bus admittance matrix; and θ_{ij} is the angle difference between the ith and the jth buses.

(ii) Voltage constraints

$$U_{i,\min} \le U_i \le U_{i,\max} \quad i \in B \quad (8)$$

where $U_{i,\min}$ and $U_{i,\max}$ are the voltage magnitude lower limit and upper limit of the ith bus, respectively, and B is the set of buses in the off-grid system.

(iii) Line flow limits

$$S_j \le S_{j,\max} \quad j \in T \quad (9)$$

where S_j is the apparent power across the jth line, $S_{j,\max}$ is the capacity limit of the jth line; and T is the set of lines in the off-grid system.

(iv) DG operation constraints

$$\alpha P_{k,R} \le P_k \le P_{k,R} \quad k \in D \quad (10)$$

$$P_k^2 + Q_k^2 \le S_{k,R}^2 \quad k \in D \quad (11)$$

$$T_k \ge T_{\min} \quad k \in D \quad (12)$$

where P_k, Q_k, $P_{k,R}$, $S_{k,R}$, and T_k are the active power output, reactive power output, rated power, rated apparent power, and continuous running time of the kth DG, respectively; α is the minimum load rate; $T_{\min}$ is the minimum running time; and D is the set of DGs in the off-grid system.

(v) BESS operation constraints

$$-P_{\mathrm{b},R} \le P_{\mathrm{b}} \le P_{\mathrm{b},R} \quad (13)$$

$$P_{\mathrm{b}}^2 + Q_{\mathrm{c}}^2 \le S_{\mathrm{c},R}^2 \quad (14)$$

$$\mathrm{SOC}_t = \mathrm{SOC}_{t-1} + \max(P_{\mathrm{b}}, 0) \cdot \eta_{\mathrm{c}} - \min(P_{\mathrm{b}}, 0)/\eta_{\mathrm{d}} \quad (15)$$

$$\mathrm{SOC}_{\min} \le \mathrm{SOC}_t \le \mathrm{SOC}_{\max} \quad (16)$$

where P_{b} and $P_{\mathrm{b},R}$ are the active power output and active power limit of battery, respectively; Q_{c} and and $S_{\mathrm{c},R}$ are the reactive power output and rated apparent power of converter, respectively; SOC_t, $\mathrm{SOC}_{\min}$, and $\mathrm{SOC}_{\max}$ are the state of charge at the tth time step, lower limit, and upper limit, respectively; and η_{c} and η_{d} are the charging and discharging efficiencies of BESS, respectively.

3.2.3 Optimal variables: In this paper, the battery energy capacity (BEC) and converter rated capacity (CRC) of the BESS are selected as optimal variables. The charge/discharge power limit of BESS is assumed to be proportional to BEC, and the ratio value is set to be 40%.

3.2.4 Model of system components: The major components in an off-grid system include DGs, WTs, battery storage, and battery converter. The models of system components, mainly refer Lambert *et al.* [23], and will not be described in this paper for the sake of conciseness.

3.3 Quasi-steady-state simulation

In this paper, the quasi-steady-state simulation includes a simulation process of components' failure and a modified strategy with power flow constraints. For a specific simulation step, first, sequential Monte Carlo simulation (SMCS) is employed to simulate the operation states of the components. Then the operation parameters, such as the number of started DGs and active power output of BESS are calculated by the hard-cycle strategy [14] and checked

IET Gener. Transm. Distrib., 2016, Vol. 10, Iss. 3, pp. 608–616

by the power flow constraints. These operation parameters will be modified if any of the constraints are not satisfied.

Similar to the SMCS, the termination criterion of quasi-steady-state simulation is the convergence of reliability index. The randomness of wind speed and uncertainty of components' failure events are considered in the simulation process and are ultimately reflected in the evaluation indices of system, as well as the operation statistics of components.

3.3.1 Simulation of components' failure: The sequential state duration sampling method is used to simulate the forced outage events of the components. For a specific component, its operation state sequence can be simulated by sampling time to failure (TTF) and time to repair (TTR).

$$\begin{cases} \text{TTF} = -a \ln R_1 \\ \text{TTR} = -b \ln R_2 \end{cases} \tag{17}$$

where a and b are the mean TTF (MTTF) and mean TTR (MTTR) of the component, respectively, and R_1 and R_2 are random numbers between 0 and 1 which follow uniform distribution.

In this paper, a failure set of DGs is established and updated, in which the generator is forced to be shut down and cannot be restarted until it is repaired. In order to reflect the overall impacts of failure events, the wind–diesel mode and wind–storage mode are added in the flow of simulation, and the system outage events caused by losing the main power supply are also considered.

When the state sequences of all the components are obtained, the network topology and operation status of the system in every time step are determined. Then the quasi-steady simulation can be carried out under certain conditions of the system.

3.3.2 Modified strategy with power flow constraints: The power conversion unit of BESS is typically a bi-directional unit capable of four-quadrant operation, which means that both real and reactive powers can be delivered or absorbed independently according to the needs of the power system [24].

When all the DGs are shut off, the BESS acts as the main power supply. Presently, the power converter works in voltage mode to meet both the active and reactive load powers. It should be noted that the BESS can not only supply active power for the load demand, but also provide reactive power to control the voltages at critical buses with the coordination of the DGs. When the DGs are started, the power conversion unit works in the current mode, in which the frequency and voltage references are given by the DGs.

The voltage in the off-grid system is related to both the active and reactive power balances due to the high resistance of distribution lines. Therefore, the impacts of active and reactive powers on the system voltage should be considered at the planning stage. In this paper, a hard-cycle strategy is adopted to determine the active power allocation of different units. Taking the impact of network topology and reactive voltage constraints into account, the operation results of hard-cycle strategy are verified by the power flow constraints and modified if any constraints are violated.

When the DGs are started, the flow of the modified strategy is as follows:

(i) Adopt the hard-cycle strategy to preliminarily determine the operation parameters, such as the number of DGs in service, the active power output of BESS, and the surplus power of WTs.

(ii) Establish the power flow equations on the basis of system operation parameters, and then solve it. If the active power requirement at the slack bus exceeds the generation capability of all started DGs, go to step iii; otherwise, go to step iv.

(iii) If the active power shortage can be offset by increasing the discharging power of BESS, regulate the active power output of BESS and go to step iv; otherwise, adopt the load shedding policy.

(iv) If the reactive power requirement at the slack bus is beyond the capability of all started DGs, go to step v; otherwise, go to step vii.

(v) If the reactive power shortage can be compensated by the reactive power capacity of BESS, regulate the reactive power output of BESS and go to step vii; otherwise, go to step vi.

(vi) If the number of started DGs equals to the maximum available number, adopt the load shedding policy. Otherwise, start a standby DG, and then repeat the whole process started from step i.

(vii) Obtain the specific information of each DG, such as power output, fuel consumption, and pollutant emissions. Update the SOC of BESS.

When the BESS acts as the system's main power supply, the modified strategy will carry out a load-shedding policy if the load demand at the slack bus exceeds the active and reactive power capacities of BESS. In this paper, a load shedding policy based on a partitioning method is adopted to divide the load nodes into blocks according to the location of isolating switches. The principle of load partitioning is as follows: for a specific isolating switch, if there is no isolating switch in its downstream feeders, all its downstream load nodes are seen as a load block; otherwise, the load nodes between the two isolating switches are regarded as a load block. All load blocks will be cut in a preset sequence which is determined by their load amount and location. If the generation capacity is still less than the load demand after all load blocks are cut off, the whole system will face an outage.

In the aforementioned modified strategy, the reactive voltage constraints are further checked and the reactive power support ability of BESS is utilised to keep the voltage stable. When severe failure events occur in the system, a load shedding policy is also adopted to recover system frequency and voltage. The modified strategy can not only obtain the power output of BESS and the operation statistics of DGs, but also acquire the outage time and unserved energy of system to provide a basis for calculating reliability indices.

3.3.3 Calculation method to obtain life cycle information: In this paper, the reliability evaluation is incorporated into the quasi-steady simulation to take components' failure events into consideration. Consequently, an alterable simulation period is adopted and the termination criterion is the convergence of the reliability index. The convergence of the simulation can be controlled by the coefficient of variation β:

$$\beta = \frac{\sqrt{V(\tilde{E}[H])}}{\tilde{E}[H]} \tag{18}$$

where $V(\tilde{E}[H])$ is the variance of the computation function $H(\text{PNS}_t)$; and $\tilde{E}[H]$ is the expected value of $H(\text{PNS}_t)$ which can be calculated based on (5).

This paper establishes the state-space model of crucial operation statistics to obtain the life cycle information. The process of building the model of DG fuel consumption is depicted in Fig. 2: First, m initial states are established and their corresponding frequencies are set to 0. Then, the state frequency is updated in each time step according to the fuel consumption. Finally, when the quasi-steady simulation is terminated, the final frequency of each state is obtained and then converted to related probability.

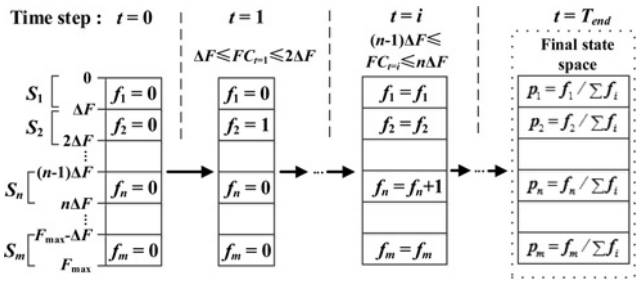

Fig. 2 *State-space model of fuel consumption*

After the state-space model of each DG is established, the total fuel consumption in the life cycle of the system can be calculated as follows:

$$\mathrm{FC}_{\mathrm{life}} = \sum_{k=1}^{m} S_k p_k \times 8760 \times L \tag{19}$$

Similarly, other crucial operation statistics in the life cycle can be calculated.

3.4 Solving algorithm

The BESS design is characterised by the BEC and CRC. The battery and converter are assumed to be integer multiples of a unit base. For example, by assuming the battery base unit equal to BU, the original optimisation range between $\mathrm{BEC}_{\min}$ and $\mathrm{BEC}_{\max}$ can assume the values [$\mathrm{BEC}_{\min}$, $\mathrm{BEC}_{\min}$ + BU, $\mathrm{BEC}_{\min}$ + 2BU, …, $\mathrm{BEC}_{\max}$]. The same way applies to the converter. The value of a base unit of the battery and converter is imposed by the tradeoff between the precision and speed of simulation.

As shown in Fig. 3, a traversal algorithm is adopted in this paper to accelerate the computation speed. On the basis of the preset parameters of the system and components, the algorithm searches the optimal solution from the lower bound to the upper bound of BEC. For each BEC, its corresponding CRC optimisation range is created according to the following principle: $\mathrm{CRC}_{\min}$ equals to the maximum active charging/discharging power of battery, and $\mathrm{CRC}_{\max}$ is determined by the required converter capacity that can meet the reactive peak load under the active power limit of the battery.

For each specific combination of BEC and CRC, the quasi-steady simulation is performed to obtain the operation statistics, such as fuel consumption and pollutant emissions until the reliability index is converged. On the basis of the obtained operation statistics and given economic parameters, the economic evaluation module is called subsequently to calculate the cash flow and pollutant emissions in the project life cycle, and then the objective function value is recorded. Finally, the optimal BEC and CRC can be determined by finding the minimum objective function value among all the feasible schemes.

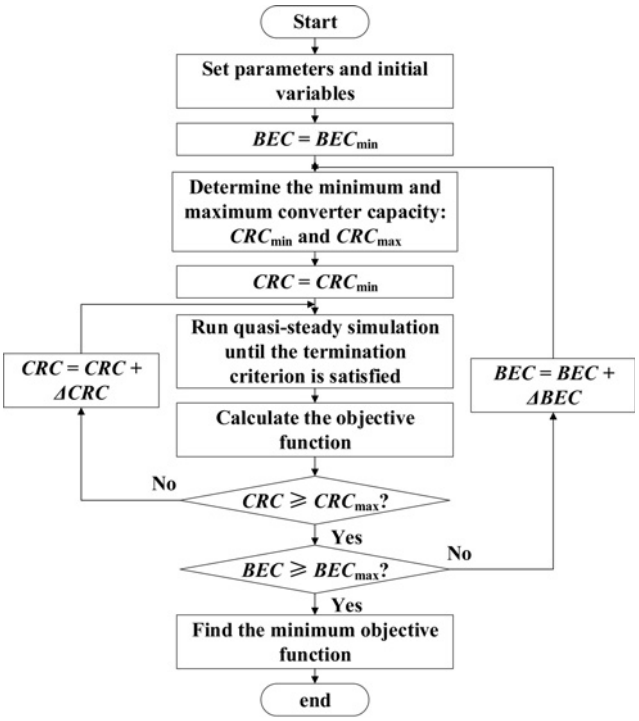

Fig. 3 *Flowchart of the solving algorithm*

4 Case study and results

The off-grid power system of Whapmagoostui community is used as a test case, as shown in Fig. 4. The Whapmagoostui community is located at the east coast of Hudson Bay, and its specific location is 55°16′N, 77°45′E. There are 400 households and 2061 CREE people in the community. Beyond the extents of electrical grid, the community has a diesel price of 1.69 C$/L and an electricity price of 1.60 C$/kWh in 2011. Three 1.4 MVA DGs are connected to the 4.16 kV bus by a set of step-up transformers in the original system. All DGs are close to their designed life span and need to be replaced. Based on feasibility research report, WTs are planned to be connected at bus #21. A BESS is located at bus #2 and its BEC and CRC are to be optimised.

The system includes two segments, each of which are protected by a recloser. Each one of the segments has no other automatic protective devices besides the re-closer and, therefore, any failure event inside leads to the isolation of the whole segment. Some manual isolating switches are set in the system, and their downstream load nodes are able to be cut off in the load shedding policy. The shedding order and peak load demand of these interruptible load blocks are shown in Table 1.

The simulation time step is set to be 1 h. In order to place emphasis on the further improvement of reliability brought by the integration of BESS meanwhile avoid losing the focus on economic benefit, the weighting coefficients of economic, environmental, and reliable indices in the objective function are selected as 0.4, 0.15, and 0.45, respectively. The coefficient of variation is chosen as 5%. Other simulation parameters are listed in Table 2, and the economic parameters are given in Table 3. It should be noted that the electricity price is set as 0.869 C$/kWh, which is far below the price of 1.60 C$/kWh when the system is only dependent on diesel generation.

In the process of synthesising time series data of wind speed, a 20 × 20 Markov process transition probability matrix is adopted.

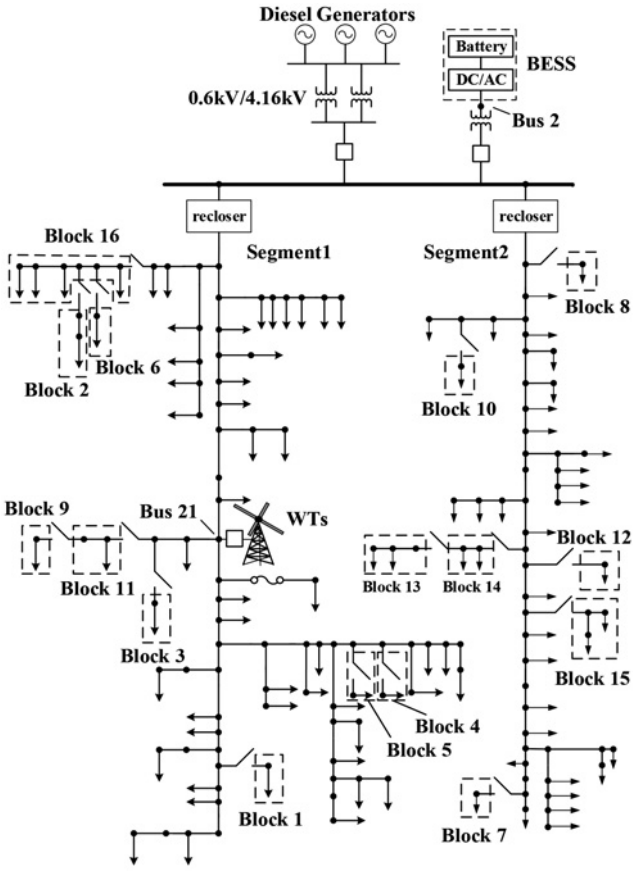

Fig. 4 *Modified system topology with WT in Quebec*

IET Gener. Transm. Distrib., 2016, Vol. 10, Iss. 3, pp. 608–616

Table 1 Shedding order of interruptible load blocks

No.	Active load, MW	Reactive load, MVar
1	0.0147	0.0037
2	0.0038	0.0013
3	0.0132	0.0034
4	0.0172	0.0043
5	0.0238	0.0056
6	0.0285	0.0094
7	0.0290	0.0095
8	0.0332	0.0064
9	0.0378	0.0092
10	0.0413	0.0089
11	0.0418	0.0070
12	0.0460	0.0109
13	0.0540	0.0117
14	0.0292	0.0067
15	0.0641	0.0138
16	0.0789	0.0176

Table 2 Simulation parameters

DG		WT	
MTTF, h	1970	MTTF, h	720
MTTR, h	100	MTTR, h	30
single rated MVA	1.4185	single rated power, kW	800
single rated MW	1.135	life, years	15
life, h	120000	hub height, m	60
minimum load rate, %	30	cut in wind speed, m/s	3
minimum running time, h	3	rated wind speed, m/s	13
emission coefficient		cut out wind speed, m/s	25
CO_2, g/L	2487	Battery	
CO, g/L	0	maximum SOC	0.9
hydrocarbon, g/L	0.07	minimum SOC	0.1
NO_x, g/L	0.07	floating charge life, years	10
SO2, L	0	maximum charge rate	1
fuel curve intercept coefficient, L	85	charge/discharge efficiency	0.9
fuel curve gradient, L/kWh	0.223	optimization range upper bound, MWh	4
System		optimization range lower bound, MWh	2
project life cycle, year	20	ratio between power limit and capacity	0.4
MTTF of each load segment, h	1440	base unit, MWh	0.2
MTTR of each load segment, h	1	Converter	
MTTF of transformer, h	0.015	life, years	20
MTTR of transformer, h	120	inversion/rectification efficiency	0.95
		base unit, MVA	0.1

Table 3 Economic parameters

DG		WT	
initial investment cost, C$	364,770	initial investment cost, C$	1,300,000
replacement cost, C$	364,770	replacement cost, C$	1,300,000
O&M cost, C$/h	75	O&M cost, C$/year	26,000
Battery		Converter	
initial investment cost, C$/kWh	482.5	initial investment cost, C$/kVA	579
replacement cost, C$/kWh	482.5	replacement cost, C$/kVA	579
O&M cost, C$/year	0	O&M cost, C$/year	0
System			
training cost, C$	1,020,000	electricity price, C$/kWh	0.869
system transforming cost, C$	3,000,000	fuel cost, C$/L (in 2013)	2.22
feasibility study cost, C$	2,678,000	discount rate, %	4
design cost, C$	1,414,000	depreciation rate, %	6.33
management cost, C$	3,468,000		

Table 4 Average monthly value of wind speed

Month	Mean of wind speed	Std of wind speed	Maximum of wind speed
1	8.2674	3.3482	19.1417
2	6.4460	3.5700	18.3917
3	6.5676	3.6024	18.7383
4	7.5210	3.8025	18.1883
5	6.2927	2.8861	14.1217
6	6.6393	3.1118	17.6883
7	7.4405	3.5111	17.2700
8	6.7785	3.2394	16.9700
9	7.2819	3.5009	19.6150
10	6.7571	3.4241	17.7717
11	8.6012	4.2667	24.8417
12	8.6438	4.4078	24.6767

The detailed information of wind speed data, including the mean value, standard deviation, and maximum value, is shown in Table 4. As for load, the total yearly active and reactive load demands in 2013 are 11,176 MWh and 3084 MVA separately. Considering the growth of electricity demand, a multiplier of 1.4 is applied to the yearly load profile in 2013. The standard deviation of daily disturbance factor and hourly distribution factor of load demand are 0.05 and 0.01, respectively.

4.1 *Effects of integrating BESS with optimal capacity*

In order to quantify the benefits associated with the optimal BESS capacity, the evaluation indices of the three cases are reported: Case 0 (diesel-only system), Case 1 (wind–diesel system with 4 WTs), and Case 2 (wind–diesel system with 4 WTs as well as the optimal BESS). The comparison of the three cases is shown in Table 5.

Table 5 Evaluation indices of Case 0, Case 1, and Case 2

Index	Case 0	Case 1	Case 2
BEC, MWh	—	—	3.4
CRC, MVA	—	—	1.5
IRR, %	— (no profit)	14.14	15.32
pollution emission, t	381,750	208,085	199,249
utilization rate of wind energy, %	—	72.32	82.14
LOEE, MWh/year	401.001	117.913	44.628
cost of generating energy, C$/kWh	1.1911	0.7701	0.7492
total running time of DG, h	396,180	1,447,210	949,300
average started number of DGs, number/h	2.261	1.652	1.084
sum of WT power, MWh	—	209,750	210,051
waste energy of WT, MWh	—	58,058	37,519
sum of DG active power, MWh	346,864	190,094	179,951
sum of DG reactive power, MWA	105,666	101,288	65,857
sum of active load, MWh	333,480	333,503	333,466
sum of reactive load, MVA	91,738	91,747	91,736
sum of battery discharging power, MWh	—	—	17,094
sum of battery charging power, MWh	—	—	23,354
sum of reactive power of BESS, MVA	—	—	36,940
annual fuel consumption, L/year	7,674,556	4,183,215	4,005,581
initial investment cost, C$	1,094,310	17,874,310	20,383,310
average annual net profit, C$/year	–5,195,030	2,523,591	3,003,033
annual revenue, C$	14,132,680	14,379,965	14,441,992
net present cost, C$	265,139,650	162,020,732	154,083,647
WT present cost, C$	—	6,747,257	6,747,257
DG present cost, C$	265,139,650	155,273,475	143,674,796
battery present cost, C$	—	—	2,793,094
converter present cost, C$	—	—	868,500

By comparing Case 0 and Case 1, it can be observed that the rational utilisation of wind energy has greatly improved the system's economic, environmental benefits, and reliability level. Due to the fuel saving brought by wind power generation, the cost of energy drops by 35.35%, and the pollution emission decreases by 45.49%. The comparison between Case 1 and Case 2 demonstrates the effects of BESS integration on the system performance. With BESS integration, all of the three main indices are further improved in Case 2. In particular, it can be seen that the system's fuel consumption drops by 4% and the average annual profit increases by 19%, which implies the huge influence of fuel cost on system's economy due to the prohibitive fuel price.

The improvement of economic and environmental objectives is mainly caused by the fact that the fuel consumption is reduced with the optimal integrated BESS. Since the interception of the DG's fuel curve is high, the fuel consumption increases notably with the started number of DGs. It should be noted that 99.99% of the pollution emission is carbon emission according to the emission coefficients, which indicates that the wind–diesel–BESS system has a significant advantage in reducing carbon emission. With BESS integrated in the system, the number of started DGs is reduced by the independent operating capability of BESS. Regarding the enhancement of system reliability, the main reason is that the reserve capacity on the generation side is increased by the discharging capability of BESS.

Fig. 5 depicts the active and reactive power balances in a typical day before and after the optimal BESS integration in the wind–diesel system (DG3 is assumed to break down). From Figs. 5*a* and *b*, it can be observed that, since the WTs are non-dispatchable generators, at least one DG must be started without the integration of BESS. Specifically, when the wind energy is abundant in the system, the active net load demand is minus but a DG is still running to meet the reactive load demand (e.g. the 10th–11th hour), which causes a serious loss of active power and fuel consumption.

However, the above problems are solved fairly well by the integration of BESS. It can be seen from Figs. 5*c* and *d* that the BESS can operate independently when the active net load demand is low (e.g. the 8th–11th hour). The reactive load demand can also be satisfied due to the reactive support ability of the bi-directional converter. In particular, when the reactive load cannot be satisfied by the current started DGs, the shortage of reactive power capacity can be offset by the BESS (e.g. the 20th hour). The simulation results provide potent support for the aforementioned conclusion that BESS reduces the number of generating DGs.

4.2 Result of changing the number of WTs

Two modified cases in which the number of WTs is 3 and 5, respectively, are investigated and compared with the base case. The evaluation indices of the optimal BESS design schemes for the three cases are summarised in Table 6. The indices of a diesel-only case are also given in Table 6 to show the superiority of wind–diesel–BESS systems. It can be observed that all the three cases with WTs and BESS outperform the diesel-only case, which proves the advantages of the wind–diesel–BESS system. The results also indicate that a larger size of WT will lead to a higher capacity of BESS. It can be observed that, although the initial investment costs are increased, the IRR of the optimal scheme for the case with five WTs is improved. That is because WTs have a low operation cost which is not subject to fuel price, and thus save a considerable amount of fuel cost to gain better profits. However, the utilisation ratio of wind energy drops sharply when additional WTs are added into the system, which becomes a main obstacle to impede the integration of more WTs into the system.

4.3 Result of changing the BESS's investment cost

To analyse the impact of BESS's initial cost, a case in which the investment cost of battery and converter are reduced by 50% is investigated and the economic indices for the base case results are

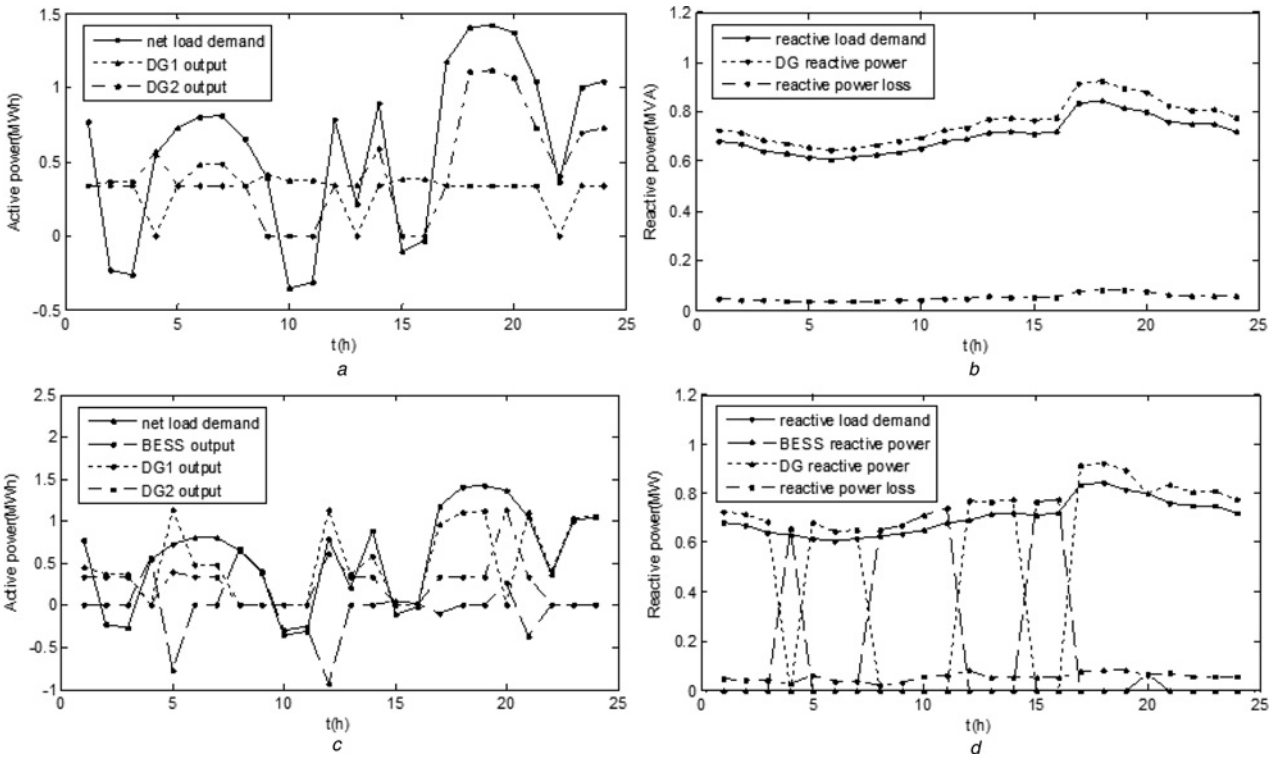

Fig. 5 *Change of system operation by the BESS integration*

a Active power balance without BESS
b Reactive power balance without BESS
c Active power balance with BESS
d Reactive power balance with BESS

IET Gener. Transm. Distrib., 2016, Vol. 10, Iss. 3, pp. 608–616

Table 6 Optimal result of different WT numbers

Index	Diesel-only	Three WTs	Four WTs	Five WTs
BEC, MWh	—	2.2	3.4	4.0
CRC, MVA	—	1.1	1.5	1.7
IRR, %	—	11.92	15.32	17.39
pollution emission, t	381,750	219,693	199,249	182,794
utilisation rate of wind energy, %	—	92.51	82.14	72.05
LOEE, MWh/year	401.001	60.081	44.628	35.54
the cost of generating energy, C$/kWh	1.1911	0.7886	0.7492	0.7185
sum of WT power, MWh	—	157,873	210,051	262,775
waste energy of WT, MWh	—	11,817	37,519	73,454
sum of DG active power, MWh	346,864	203,195	179,951	164,159
sum of battery discharging power, MWh	—	7502	17,094	20,624
sum of battery charging power, MWh	—	10,225	23,354	28,192
annual fuel consumption, L/year	7,674,556	4,416,582	4,005,581	3,674,775
initial investment cost, C$	1,094,310	18,272,710	20,383,310	22,088,610
average annual net profit, C$/year	–5,195,030	2,240,634	3,003,033	3,599,950
battery present cost, C$	—	1,807,296	2,793,094	3,285,992
converter present cost, C$	—	636,900	868,500	984,300

Table 7 Comparison between the new and original result

Index	New optimal result	Original optimal result
BEC, MWh	3.8	3.4
CRC, MVA	1.7	1.5
IRR, %	15.94	16.82
pollution emission, t	201,977	199,249
utilisation rate of wind energy, %	82.86%	82.14
LOEE, MWh/year	41.809	44.628
sum of battery discharging power, MWh	20,984	17,094
sum of battery charging power, MWh	28,678	23,354
sum of reactive power of BESS, MVA	39,053	36,940
initial investment cost, C$	19,283,210	19,128,810
average annual net profit, C$/year	2,979,845	3,106,770
battery present cost, C$	1,560,846	1,396,547
converter present cost, C$	492,150	434,250

recalculated. Table 7 shows the comparison between the new and original optimal BESS capacity.

It can be seen that the IRR of the original case is increased with reduced initial cost. Comparing to the original case, the optimal capacity of the BESS is higher in the new case, but the economy becomes worse while the reliability level is improved. It can be concluded that the optimal capacity of BESS is highly sensitive to the changes of BESS prices. When the initial cost of BESS is high, the cost of reliability improvement is so exorbitant that it is unfeasible to install high capacity BESS to achieve better reliability. However, when the cost of BESS drops to a certain level, a higher-capacity BESS with higher reliable level may become practicable for the wind–diesel off-grid system.

5 Conclusions

In this paper, an optimal planning model for the capacity of BESS aiming at maximising the economic, environmental benefits, and reliability level for a wind–diesel off-grid system is proposed in the proposed method. Also, a quasi-steady state simulation considering the randomness of renewable energy, the uncertainty of components failure events, and the power flow constraints is adopted. The optimal design of BESS has been carried out for the wind–diesel off-grid power system in the Whapmagoostui community, and the integration effects of BESS has been analysed through a comparative case study. The principle conclusions are as follows:

(i) The proper design of the BESS in a wind–diesel off-grid system with high fuel prices enhances system economic, environmental benefits, and reliability, as demonstrated in this paper. The economic improvement is mainly due to the fuel cost saving caused by the remarkable reduction of DGs' total running time. When the RER is abundant and the fuel price is prohibitive, it is an efficient alternative to integrate BESS into the system.

(ii) The ability of BESS to regulate both the active and reactive powers improves the performance of the wind–diesel off-grid power system. The BESS is able to operate independently and thus reduce the burden of DGs. The number of started DGs decreases significantly with the integration of BESS.

(iii) A larger number of WTs leads to a higher capacity of BESS. The combination scheme of more WTs and higher-capacity BESS may achieve better economy and reliability, but the feasibility is limited by the low wind energy utilisation rate. Besides, if the initial investment cost of battery and converter declines, a higher-capacity BESS with a good reliability level will become a practical solution.

6 Acknowledgments

The authors greatly appreciate the financial supports from the National Nature Science Foundation of China (Project No. 51207099), the adaption and grid connection technology research of distributed generation in distribution systems of State Grid Corporation of China, and the facility support provided by CURENT which is a NSF and DOE Engineering Research Center funded under NSF Grant EEC-1041877.

7 References

1 'Aboriginal Affairs and Northern Development Canada, Off-Grid Communities', https://www.aadnc-aandc.gc.ca/eng/1314295992771/1314296121126, accessed May 2012
2 Arriaga, M., Canizares, C.A., Kazerani, M.: 'Renewable energy alternatives for remote communities in northern Ontario, Canada', *IEEE Trans. Sustain. Energy*, 2013, **4**, (3), pp. 661–670
3 Arriaga, M., Canizares, C.A., Kazerani, M.: 'Northern lights: access to electricity in Canada's northern and remote communities', *IEEE Power Energ. Mag.*, 2014, **12**, (4), pp. 50–59
4 'Natural Resources Canada, About Renewable Energy', http://www.nrcan.gc.ca/energy/renewable-electricity/7295#wind, accessed April 2014
5 Weis, T.M., Ilinca, A.: 'Assessing the potential for a wind power incentive for remote villages in Canada', *Energy Policy*, 2010, **38**, (10), pp. 5504–5511
6 Fay, G., Udovyk, N.: 'Factors influencing success of wind-diesel hybrid systems in remote Alaska communities: results of an informal survey', *Renew. Energy*, 2013, **57**, pp. 554–557
7 Weis, T.M., Ilinca, A., Pinard, J.P.: 'Stakeholders' perspectives on barriers to remote wind–diesel power plants in Canada', *Energy Policy*, 2008, **36**, pp. 1611–1621
8 Bowen, A.J., Cowie, M., Zakay, N.: 'The performance of a remote wind–diesel power system', *Renew. Energy*, 2001, **22**, pp. 429–445
9 Bo, Z., Xuesong, Z., Peng, L., Ke, W., Meidong, X., Caisheng, W.: 'Optimal sizing, operating strategy and operational experience of a stand-alone microgrid on Dongfushan Island', *Appl. Energy*, 2014, **113**, pp. 1656–1666
10 Bo, Z., Xuesong, Z., Jian, C., Caisheng, W., Li, G.: 'Operation optimization of standalone microgrids considering lifetime characteristics of battery energy storage system', *IEEE Trans. Sustain. Energy*, 2013, **4**, (4), pp. 934–943
11 Dufo-López, R., Bernal-Agustín, J.L., Yusta-Loyo, J.M., *et al.*: 'Multi-objective optimization minimizing cost and life cycle emissions of stand-alone PV-wind-diesel systems with batteries storage', *Appl. Energy*, 2011, **88**, (11), pp. 4033–4041
12 Dufo-Lopez, R., Bernal-Agustin, J.L.: 'Multi-objective design of PV–wind–diesel–hydrogen –battery systems', *Renew. Energy*, 2008, **33**, (12), pp. 2559–2572
13 Changsong, C., Shanxu, D.: 'Optimal allocation of distributed generation and energy storage system in microgrids', *IET Renew. Power Gener.*, 2014, **8**, (6), pp. 581–589

14 Li, G., Wenjian, L., Bingqi, J., Bowen, H., Chengshan, W.: 'Multi-objective stochastic optimal planning method for stand-alone microgrid system', *IET Gener. Transm. Distrib.*, 2014, **8**, (7), pp. 1263–1273
15 Nick, M., Cherkaoui, R., Paolone, M.: 'Optimal allocation of dispersed energy storage systems in active distribution networks for energy balance and grid support', *IEEE Trans. Power Syst.*, 2014, **29**, (5), pp. 2300–2310
16 Atwa, Y.M., El-Saadany, E.F.: 'Optimal allocation of ESS in distribution systems with a high penetration of wind energy', *IEEE Trans. Power Syst.*, 2010, **25**, (4), pp. 1815–1822
17 Awad, A.S.A., EL-Fouly, T.H.M., Salama, M.M.A.: 'Optimal ESS allocation and load shedding for improving distribution system reliability', *IEEE Trans. Smart Grid*, 2014, **5**, (5), pp. 2339–2349
18 Carpineli, G., Celli, G., Mocci, S., Mottola, F., Pilo, F., Proto, D.: 'Optimal integration of distributed energy storage devices in smart grids', *IEEE Trans. Smart Grid*, 2013, **4**, (2), pp. 985–995
19 Manwell, J.F., Rogers, A., Hayman, G., *et al.*: 'Hybrid2: a hybrid system simulation model: theory manual' (National Renewable Energy Laboratory, Colorado, 1998)
20 Blaabjerg, F., Zhe, C., Kjaer, S.B.: 'Power electronics as efficient interface in dispersed power generation systems', *IEEE Trans. Power Electron.*, 2004, **19**, (5), pp. 1184–1194
21 Vinothkumar, K., Selvan, M.P.: 'Fuzzy embedded genetic algorithm method for distributed generation planning', *Elect. Power Compon. Syst.*, 2011, **39**, (4), pp. 346–366
22 Shadmand, M.B., Balog, R.S.: 'Multi-objective optimization and design of photovoltaic-wind hybrid system for community smart DC microgrid', *IEEE Trans. Smart Grid*, 2014, **5**, (5), pp. 2635–2643
23 Lambert, T., Gilman, P., Lilienthal, P.: 'Micropower system modeling with HOMER' (Wiley-IEEE Press, New York, 2006)
24 Hill, C.A., Such, M.C., Dongmei, C., Gonzalez, J., Grady, W.M.: 'Battery energy storage for enabling integration of distributed solar power generation', *IEEE Trans. Smart Grid*, 2012, **3**, (2), pp. 850–857